A model for coupling reservoir inflow and wellbore flow in fishbone wells

Lian Peiqing[1, 2], Cheng Linsong[2]*, Tan Xuequn[1] and Li Linlin[1]

© China University of Petroleum (Beijing) and Springer-Verlag Berlin Heidelberg 2012

[1] Sinopec Petroleum Exploration and Production Research Institute, Beijing 100083, China
[2] School of Petroleum Engineering, China University of Petroleum (Beijing), Beijing 102249, China

Abstract: A coupling model is proposed in this paper by using the Green Function and Newman's product principle, and the solution method is provided here as well. This model can be used to describe the reservoir inflow and wellbore flow for fishbone wells in an unsteady flow or pseudo-steady flow state. A case study indicates that the bottom hole pressure declines quickly in the unsteady flow period which is very short. The pressure drop per unit time remains unchanged under the pseudo-steady flow conditions. The distribution of flow rate along the main wellbore shows a wave shape under the unsteady flow condition, and the flow rate distribution in each branch is similar. The flow rate distribution along the main wellbore is irregular "U" shaped under the pseudo-steady flow condition, and the space-symmetrical branches have the same flow distribution pattern. In the initial production period, the flow rate increases significantly as the length of branches and the angle between branches and the main wellbore increase. As the production continues, the length and angle of branches have only a slight effect on the flow in fishbone wells.

Key words: Fishbone wells, coupling model, unsteady flow state, pseudo-steady flow state

1 Introduction

The use of multilateral horizontal wells can greatly increase the reservoir drainage volume and effectively control water/gas coning, and hence enhance the recovery of low-permeability reservoirs. As a result, this technique has become a popular research topic in recent years (Jasti et al, 1997; Lian et al, 2011; Salas et al, 1996; Wang et al, 2006; 2010; Zhang et al, 2011). Fishbone wells, as one of the typical multilateral horizontal well types, can effectively improve the single well controlled reserves and reduce the number of development wells as well as the development cost. Much research has been done on fishbone well productivity and pressure distribution. Li and Zhang (2010) obtained the productivity equation of fishbone wells by the equivalent flow resistance method, and calculated the productivity of horizontal wells. Liu et al (2000) proposed a model to describe the 3-dimensional pressure distribution during the production of fishbone wells on the basis of the 3-dimensional steady flow in the reservoir and the characteristics of fluid flow in multilateral horizontal wells. He et al (2004) and Fan et al (2006) used the node method to calculate the steady-state productivity of fishbone wells after dividing the wellbore into flow segments. Yi et al (2008) applied the technique of fishbone wells in heavy oil reservoirs, and eventually achieved an enhanced oil recovery.

Taking six herringbone wells in one oil field in Bohai as samples, Jiang et al (2011) and Ye et al (2010) constructed a back-propagation (BP) neural network model to predict the herringbone well productivity which is affected by multifactorial and nonlinear conditions. Huang et al (2010) on the basis of the 3-D spatial description of the fishbone well trajectory, built a new percolation model around the fishbone well production section, which is limited by closed upper and lower boundaries. Yu et al (2009) investigated the possibility of using fishbone wells to maximize the net-present value (NPV) during the field development, and concluded that the use of fishbone wells with increased number of rib holes would be more beneficial than multi-fractured wells when developing tight gas reservoirs.

Nowadays, the research on fishbone wells with steady-state flow is well developed. However, most of these theories cannot be used to describe the pressure and flow distribution during the transient flow period. Based on above research, this paper superimposes the pressure in space and time to establish a fishbone well transient flow model, which can be applied in both unsteady and pseudo-steady flow conditions.
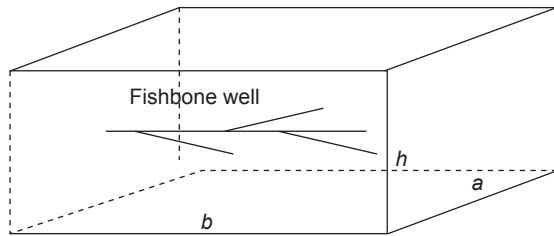
2 Model development

2.1 Assumptions

1) The reservoir is heterogeneous, with six external closed boundaries. The reservoir permeability in the x, y and z directions are k_x, k_y, and k_z. The porosity is ϕ, and the initial
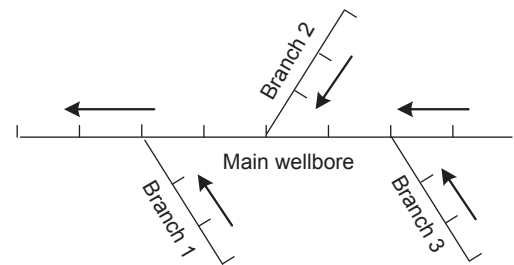
pressure is p_{ini}.

2) As is shown in Fig. 1, a fishbone well, which has n branches, is placed in this reservoir with random length, angle and location.

3) The single-phase fluid in this reservoir is slightly compressible.

4) The fluid flows isothermally within the whole reservoir.

(a) 3-D dimension

(b) Plan view

Fig. 1 Schematic diagram of a fishbone well

2.2 Nodal flow model

The governing equation for the slightly compressible fluid flow in elastic porous media can be expressed as:

$$K_x \frac{\partial^2 p}{\partial x^2} + K_y \frac{\partial^2 p}{\partial y^2} + K_z \frac{\partial^2 p}{\partial z^2} = \phi \mu C_t \frac{\partial p}{\partial t} \qquad (1)$$

It is assumed that a point-sink is located at the coordinates (x_i, y_i, z_i) and produces at a unit rate. At time t, the pressure drop at (x_i, y_i, z_i) is denoted by $F_{i,j}(t)$, and it can be expressed as (Ouyang and Aziz, 1998):

$$F_{i,j} = p_{ini} - p((x_i, y_i, z_i); (x_j, y_j, z_j); t) \qquad (2)$$

where $p((x_i, y_i, z_i); (x_j, y_j, z_j); t)$ is the pressure at time t, at position (x_i, y_i, z_i).

By applying the superposition principle in space, one can obtain the pressure drop at (x_i, y_i, z_i) when several nodes at (x_i, y_i, z_i) yield simultaneously:

$$\Delta p_i = p_{ini} - \sum_{j=1}^{n} p((x_i, y_i, z_i); (x_j, y_j, z_j); t)$$
$$= \sum_{j=1}^{n} F_{i,j}(t) q_j(t) \qquad (3)$$

where q_j is the time-independent flow rate of the j-th node.

For the case of the variable mass flow at each node, the pressure drop at random position (x_i, y_i, z_i) can be obtained by using the Duhamel theorem:

$$\Delta p_i = \int_0^t \sum_{j=1}^{n} q_j(t-\tau) \left[-\frac{\mathrm{d}F_{i,j}(\tau)}{\mathrm{d}\tau} \right] \mathrm{d}\tau \qquad i=1, 2, \cdots, n \qquad (4)$$

By considering the horizontal well as a line sink and integrating Eq. (4), one can obtain the pressure drop when several wells produce at the same time.

2.3 A model to couple wellbore flow and reservoir inflow for fishbone wells

At time $t = 0^+$, one well branch produces at a rate of q. The well extends from (x_1, y_1, z_0) to (x_2, y_2, z_0). Thus, the length L is equal to $\sqrt{(x_2 - x_1)^2 + (y_2 - y_1)^2}$. Each point on

the branch can be given as:

$$\begin{cases} x = x_1 + R\sin\theta \\ y = y_1 + R\cos\theta \\ z = z_0 \end{cases} \qquad (5)$$

where θ is the angle between the branch and the y axis; R is the distance between one point on the well and the point (x_1, y_1, z_0).

Therefore, by using Newman's product principle, the pressure drop caused by the production of the branch at random location (x, y, z) and random time $(t > 0)$ is given as (Babu and Odeh, 1988; Penmatcha and Aziz, 1998):

$$p_i - p(x, y, z, t) = q \cdot F(x, y, z, t)$$
$$= \frac{q}{\phi C_t L} \cdot \int_0^t \int_0^L (S_1 \cdot S_2 \cdot S_3) \, \mathrm{d}R \, \mathrm{d}\tau \qquad (6)$$

with
$$S_1 = S_1(x, R, t)$$
$$= \frac{1}{a} \left[1 + 2\sum_{n=1}^{\infty} \cos\frac{n\pi x}{a} \cos\frac{n\pi(x_1 + R\sin\theta)}{a} \exp\left(-\frac{n^2\pi^2 K_x t}{\alpha a^2}\right) \right]$$

$$S_2 = S_2(y, R, t)$$
$$= \frac{1}{b} \left[1 + 2\sum_{m=1}^{\infty} \cos\frac{m\pi y}{b} \cos\frac{m\pi(y_1 + R\cos\theta)}{b} \exp\left(-\frac{m^2\pi^2 K_y t}{\alpha b^2}\right) \right]$$

$$S_3 = S_3(z, z_0, t)$$
$$= \frac{1}{h} \left[1 + 2\sum_{l=1}^{\infty} \cos\frac{l\pi z}{h} \cos\frac{l\pi z_0}{h} \exp\left(-\frac{l^2\pi^2 K_z t}{\alpha h^2}\right) \right]$$

where $\alpha = \phi\mu C_t$, and S_1, S_2, and S_3 are Green's functions located at $(x_1 + R\sin\theta, y_1 + R\cos\theta, z_0)$.

It is assumed that the fishbone well has n branches. The main wellbore is divided into s_0 segments, and the i-th segment is divided into s_i smaller segments. Then, there are totally $s_0 + s_1 + s_2 + \cdots + s_n$ small segments, which can be considered as small horizontal wells. The pressure equation

shown as Eq. (6) can be applied to each small horizontal segment. When superposing the pressure in different space, we should consider the interference between each segment. As Fig. 2 shows, the node of each horizontal segment locates in the center of each segment and is on the axis of wellbore. The reservoir node is on the wellbore, and the distance between this node and the wellbore node is r_w. We can write:

$$n_s = s_0 + s_1 + s_2 + \cdots + s_n \tag{7}$$

There are totally $3n_s$ unknown variables:

Fig. 2 Segments division (taking the main wellbore as an example)

1) Reservoir nodes pressure: $p_1, p_2, \cdots, p_{s_0}$; $p_{1,1}, p_{1,2}, \cdots, p_{1,s_1}$; $\cdots$; $p_{n,1}, p_{n,2}, \cdots, p_{n,s_n}$;

2) Segment nodes pressure: $p_{w,1}, p_{w,2}, \cdots, p_{w,s_0}$; $p_{w,1,1}, p_{w,1,2}, \cdots, p_{w,1,s_1}$; $\cdots$; $p_{w,n,1}, p_{w,n,2}, \cdots, p_{w,n,s}$;

3) Flow rate from reservoir nodes to segment nodes: $q_1, q_2, \cdots, q_{s_0}$; $q_{1,1}, q_{1,2}, \cdots, q_{1,s_1}$; $\cdots$; $q_{n,1}, q_{n,2}, \cdots, q_{n,s_n}$.

Continuity equation of pressure: At the m-th time step, to maintain the pressure continuity between the reservoir and the wellbore, the relationship between the reservoir pressure and the wellbore node pressure is as follows:

$$\text{Main wellbore: } p_j(m\Delta t) = p_{w,j}(m\Delta t) + \frac{S_j q_j(m\Delta t)\mu B}{2\pi\sqrt{K_x K_z}L} \tag{8}$$

$$\text{Branch: } p_{i,j}(m\Delta t) = p_{w,i,j}(m\Delta t) + \frac{S_{i,j}q_{i,j}(m\Delta t)\mu B}{2\pi\sqrt{K_x K_z}L} \tag{9}$$

where L is the length of small horizontal segments, and S is the skin factor of the horizontal segment.

Flow equation: The flow equation is obtained by superimposing all segments in space and time. At the m-th time step, the i-th segment of the main wellbore is written as:

$$
\begin{aligned}
&p_{\text{ini}} - p_i(m\Delta t) \\
&= \sum_{s=1}^{s_0}\left(q_s(\Delta t)F_{i,s}(m\Delta t) + \sum_{k=2}^{m}(q_s(k\Delta t) - q_s((k-1)\Delta t))F_{i,s}((m-k+1)\Delta t) \right) \\
&+ \sum_{u=1}^{n}\sum_{v=1}^{s_u}\left(q_{u,v}(\Delta t)F_{i,(u,v)}(m\Delta t) + \sum_{k=2}^{m}(q_{u,v}(k\Delta t) - q_{u,v}((k-1)\Delta t))F_{i,(u,v)}((m-k+1)\Delta t) \right)
\end{aligned}
\tag{10}
$$

where $F_{i,s}$ represents the effect of the s-th segment of the main wellbore on its i-th segment, and $F_{i,(u,v)}$ represents the effect of the v-th segment of the u-th branch on the i-th segment. There are totally s_0 equations of such kind.

At the m-th time step, the flux equation of the j-th segment of the i-th branch is as follows:

$$
\begin{aligned}
p_{\text{ini}} - p_{i,j}(m\Delta t) &= \sum_{s=1}^{s_0}\left(q_s(\Delta t)F_{(i,j),s}(m\Delta t) + \sum_{k=2}^{m}(q_s(k\Delta t) - q_s((k-1)\Delta t))F_{(i,j),s}((m-k+1)\Delta t) \right) \\
&+ \sum_{u=1}^{n}\sum_{v=1}^{s_u}\left(q_{u,v}(\Delta t)F_{(i,j),(u,v)}(m\Delta t) + \sum_{k=2}^{m}(q_{u,v}(k\Delta t) - q_{u,v}((k-1)\Delta t))F_{(i,j),(u,v)}((m-k+1)\Delta t) \right)
\end{aligned}
\tag{11}
$$

where $F_{(i,j),s}$ shows the effect of the s-th segment of the main wellbore on the j-th segment of the i-th branch, and $F_{(i,j),(u,v)}$ shows the effect of the v-th segment of the u-th branch on the j-th segment of the i-th branch. There are totally $n_s - s_0$ equations of such kind.

Wellbore model: Generally, the pressure drop in the wellbore is small. Therefore, if the pressure drop, compared with the producing pressure drop, is small enough to be ignored, the wellbore can be assumed as an infinite-conductive one, and the following equations can be obtained:

$$p_{w,1} = p_{w,2} = \cdots = p_{w,n} = p_{w,1,1} = p_{w,1,2} = \cdots = p_{w,1,s_1} = \cdots = p_{w,n,1} = p_{w,n,2} = \cdots = p_{w,n,s_n} \tag{12}$$

Constraint equation: The model can be constrained by flux or bottom hole pressure to build equations as follows:
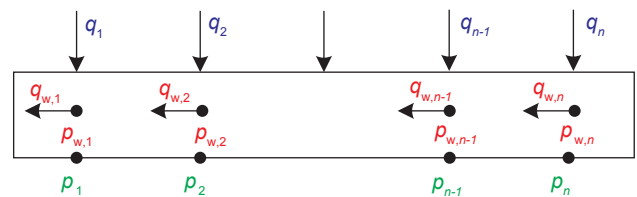Flux constraint:

$$\sum_{i=1}^{s_0} q_i + \sum_{i=1}^{n}\sum_{j=1}^{s_i} q_{i,j} - Q_T = 0 \tag{13}$$

Bottom hole pressure constraint: $p_{w,1} - p_{wf} = 0$ \hfill (14)

where Q_T represents the expected maximum flux; and p_{wf} represents the known bottom hole pressure, MPa.

3 Solving method

In the developed model, there are totally $3n_s$ unknowns and $3n_s$ equations (Eqs. (8), (9), (10), (11), (12), (13) or (14)). In the solution process, the continuity equation of pressure and wellbore model can be used to eliminate the variables of reservoir and well segment node pressure. And then, there are only n_s+1 unknowns to solve, including the wellbore pressure p and the node flow rate from reservoir node to segment node ($q_1, q_2, ..., q_{s_0}; q_{1,1}, q_{1,2}, ..., q_{1,s_1}; \cdots, q_{n,1}, q_{n,2}, ..., q_{n,s_n}$), which can be solved by a set of n_s+1 equations (Eqs. (10), (11), (13) or (14)).

Eq. (10) can be transformed into the following expression:

$$\sum_{s=1}^{s_0} q_s(m\Delta t)F_{i,s}(\Delta t) + \sum_{u=1}^{n}\sum_{v=1}^{s_u} q_{u,v}(m\Delta t)F_{i,(u,v)}(\Delta t) - [p_{ini} - p(m\Delta t)]$$
$$= -\sum_{s=1}^{s_0}\sum_{k=1}^{m-1} q_s(k\Delta t)[F_{i,s}((m-k+1)\Delta t) - F_{i,s}((m-k)\Delta t)] - \sum_{u=1}^{n}\sum_{v=1}^{s_u}\sum_{k=1}^{m-1} q_{u,v}(k\Delta t)[F_{i,(u,v)}((m-k+1)\Delta t) - F_{i,(u,v)}((m-k)\Delta t)] \tag{15}$$

Similarly, Eq. (11) can be transformed into the following expression:

$$\sum_{s=1}^{s_0} q_s(m\Delta t)F_{(i,j),s}(\Delta t) + \sum_{u=1}^{n}\sum_{v=1}^{s_u} q_{u,v}(m\Delta t)F_{(i,j),(u,v)}(\Delta t) - [p_{ini} - p(m\Delta t)]$$
$$= -\sum_{s=1}^{s_0}\sum_{k=1}^{m-1} q_s(k\Delta t)[F_{(i,j),s}((m-k+1)\Delta t) - F_{(i,j),s}((m-k)\Delta t)] - \sum_{u=1}^{n}\sum_{v=1}^{s_u}\sum_{k=1}^{m-1} q_{u,v}(k\Delta t)[F_{(i,j),(u,v)}((m-k+1)\Delta t) - F_{(i,j),(u,v)}((m-k)\Delta t)] \tag{16}$$

If we use the flux constraint equation, the solving equation can be written as a matrix expression:

$$\begin{bmatrix} F_{1,1} & F_{1,2} & \cdots & F_{1,s_0} & F_{1,(1,1)} & F_{1,(1,2)} & \cdots & F_{1,(1,s_1)} & \cdots & F_{1,(n,1)} & F_{1,(n,2)} & \cdots & F_{1,(n,s_n)} & -1 \\ F_{2,1} & F_{2,2} & \cdots & F_{2,s_0} & F_{2,(1,1)} & F_{2,(1,2)} & \cdots & F_{2,(1,s_1)} & \cdots & F_{2,(n,1)} & F_{2,(n,2)} & \cdots & F_{2,(n,s_n)} & -1 \\ \cdots & \cdots & \cdots & \cdots & \cdots & \cdots & \cdots & \cdots & \cdots & \cdots & \cdots & \cdots & \cdots & \cdots \\ F_{s_0,1} & F_{s_0,2} & \cdots & F_{s_0,s_0} & F_{s_0,(1,1)} & F_{s_0,(1,2)} & \cdots & F_{s_0,(1,s_1)} & \cdots & F_{s_0,(n,1)} & F_{s_0,(n,2)} & \cdots & F_{s_0,(n,s_n)} & -1 \\ F_{(1,1),1} & F_{(1,1),2} & \cdots & F_{(1,1),s_0} & F_{(1,1),(1,1)} & F_{(1,1),(1,2)} & \cdots & F_{(1,1),(1,s_1)} & \cdots & F_{(1,1),(n,1)} & F_{(1,1),(n,2)} & \cdots & F_{(1,1),(n,s_n)} & -1 \\ F_{(1,2),1} & F_{(1,2),2} & \cdots & F_{(1,2),s_0} & F_{(1,2),(1,1)} & F_{(1,2),(1,2)} & \cdots & F_{(1,2),(1,s_1)} & \cdots & F_{(1,2),(n,1)} & F_{(1,2),(n,2)} & \cdots & F_{(1,2),(n,s_n)} & -1 \\ \cdots & \cdots & \cdots & \cdots & \cdots & \cdots & \cdots & \cdots & \cdots & \cdots & \cdots & \cdots & \cdots & \cdots \\ F_{(1,s_0),1} & F_{(1,s_0),2} & \cdots & F_{(1,s_0),s_0} & F_{(1,s_0),(1,1)} & F_{(1,s_0),(1,2)} & \cdots & F_{(1,s_0),(1,s_1)} & \cdots & F_{(1,s_0),(n,1)} & F_{(1,s_0),(n,2)} & \cdots & F_{(1,s_0),(n,s_n)} & -1 \\ \cdots & \cdots & \cdots & \cdots & \cdots & \cdots & \cdots & \cdots & \cdots & \cdots & \cdots & \cdots & \cdots & \cdots \\ F_{(n,1),1} & F_{(n,1),2} & \cdots & F_{(n,1),s_0} & F_{(n,1),(1,1)} & F_{(n,1),(1,2)} & \cdots & F_{(n,1),(1,s_1)} & \cdots & F_{(n,1),(n,1)} & F_{(n,1),(n,2)} & \cdots & F_{(n,1),(n,s_n)} & -1 \\ F_{(n,2),1} & F_{(n,2),2} & \cdots & F_{(n,2),s_0} & F_{(n,2),(1,1)} & F_{(n,2),(1,2)} & \cdots & F_{(n,2),(1,s_1)} & \cdots & F_{(n,2),(n,1)} & F_{(n,2),(n,2)} & \cdots & F_{(n,2),(n,s_n)} & -1 \\ \cdots & \cdots & \cdots & \cdots & \cdots & \cdots & \cdots & \cdots & \cdots & \cdots & \cdots & \cdots & \cdots & \cdots \\ F_{(n,n),1} & F_{(n,n),2} & \cdots & F_{(n,n),s_0} & F_{(n,n),(1,1)} & F_{(n,n),(1,2)} & \cdots & F_{(n,n),(1,s_1)} & \cdots & F_{(n,n),(n,1)} & F_{(n,n),(n,2)} & \cdots & F_{(n,n),(n,s_n)} & -1 \\ 1 & 1 & \cdots & 1 & 1 & 1 & \cdots & 1 & \cdots & 1 & 1 & \cdots & 1 & 0 \end{bmatrix} \begin{bmatrix} q_1^m \\ q_2^m \\ \cdots \\ q_{s_0}^m \\ q_{1,1}^m \\ q_{1,2}^m \\ \cdots \\ q_{1,s_1}^m \\ \cdots \\ q_{n,1}^m \\ q_{n,2}^m \\ \cdots \\ q_{n,s_n}^m \\ \Delta p^m \end{bmatrix} = \begin{bmatrix} r_1^{m-1} \\ r_2^{m-1} \\ \cdots \\ r_{s_0}^{m-1} \\ r_{1,1}^{m-1} \\ r_{1,2}^{m-1} \\ \cdots \\ r_{1,s_1}^{m-1} \\ \cdots \\ r_{n,1}^{m-1} \\ r_{n,2}^{m-1} \\ \cdots \\ r_{n,s_n}^{m-1} \\ Q_{max} \end{bmatrix} \tag{17}$$

where $\Delta p^m = p_{ini} - p(m\Delta t)$, $q_i^m = q_i(m\Delta t)$, $q_{i,j}^m = q_{i,j}(m\Delta t)$, r_i^{m-1} is the term on the right-hand side of Eq. (15), $r_{i,j}^{m-1}$ is the term on the right-hand side of Eq. (16), and the unknown variable are Δp^m, $q_1^m, q_2^m, \cdots, q_{s_0}^m$, $q_{1,1}^m, q_{1,2}^m, \cdots, q_{1,s_1}^m, \cdots, q_{n,1}^m, q_{n,2}^m, \cdots, q_{n,s_n}^m$.

If we use the bottom hole pressure constraint equation, the Δp^m will be known, and the solving equation can be written as an matrix expression:

$$
\begin{bmatrix}
F_{1,1} & F_{1,2} & \cdots & F_{1,s_0} & F_{1,(1,1)} & F_{1,(1,2)} & \cdots & F_{1,(1,s_1)} & \cdots & F_{1,(n,1)} & F_{1,(n,2)} & \cdots & F_{1,(n,s_n)} & 0 \\
F_{2,1} & F_{2,2} & \cdots & F_{2,s_0} & F_{2,(1,1)} & F_{2,(1,2)} & \cdots & F_{2,(1,s_1)} & \cdots & F_{2,(n,1)} & F_{2,(n,2)} & \cdots & F_{2,(n,s_n)} & 0 \\
\cdots & \cdots & \cdots & \cdots & \cdots & \cdots & \cdots & \cdots & \cdots & \cdots & \cdots & \cdots & \cdots & \cdots \\
F_{s_0,1} & F_{s_0,2} & \cdots & F_{s_0,s_0} & F_{s_0,(1,1)} & F_{s_0,(1,2)} & \cdots & F_{s_0,(1,s_1)} & \cdots & F_{s_0,(n,1)} & F_{s_0,(n,2)} & \cdots & F_{s_0,(n,s_n)} & 0 \\
F_{(1,1),1} & F_{(1,1),2} & \cdots & F_{(1,1),s_0} & F_{(1,1),(1,1)} & F_{(1,1),(1,2)} & \cdots & F_{(1,1),(1,s_1)} & \cdots & F_{(1,1),(n,1)} & F_{(1,1),(n,2)} & \cdots & F_{(1,1),(n,s_n)} & 0 \\
F_{(1,2),1} & F_{(1,2),2} & \cdots & F_{(1,2),s_0} & F_{(1,2),(1,1)} & F_{(1,2),(1,2)} & \cdots & F_{(1,2),(1,s_1)} & \cdots & F_{(1,2),(n,1)} & F_{(1,2),(n,2)} & \cdots & F_{(1,2),(n,s_n)} & 0 \\
\cdots & \cdots & \cdots & \cdots & \cdots & \cdots & \cdots & \cdots & \cdots & \cdots & \cdots & \cdots & \cdots & \cdots \\
F_{(1,s_0),1} & F_{(1,s_0),2} & \cdots & F_{(1,s_0),s_0} & F_{(1,s_0),(1,1)} & F_{(1,s_0),(1,2)} & \cdots & F_{(1,s_0),(1,s_1)} & \cdots & F_{(1,s_0),(n,1)} & F_{(1,s_0),(n,2)} & \cdots & F_{(1,s_0),(n,s_n)} & 0 \\
\cdots & \cdots & \cdots & \cdots & \cdots & \cdots & \cdots & \cdots & \cdots & \cdots & \cdots & \cdots & \cdots & \cdots \\
F_{(n,1),1} & F_{(n,1),2} & \cdots & F_{(n,1),s_0} & F_{(n,1),(1,1)} & F_{(n,1),(1,2)} & \cdots & F_{(n,1),(1,s_1)} & \cdots & F_{(n,1),(n,1)} & F_{(n,1),(n,2)} & \cdots & F_{(n,1),(n,s_n)} & 0 \\
F_{(n,2),1} & F_{(n,2),2} & \cdots & F_{(n,2),s_0} & F_{(n,2),(1,1)} & F_{(n,2),(1,2)} & \cdots & F_{(n,2),(1,s_1)} & \cdots & F_{(n,2),(n,1)} & F_{(n,2),(n,2)} & \cdots & F_{(n,2),(n,s_n)} & 0 \\
\cdots & \cdots & \cdots & \cdots & \cdots & \cdots & \cdots & \cdots & \cdots & \cdots & \cdots & \cdots & \cdots & \cdots \\
F_{(n,n),1} & F_{(n,n),2} & \cdots & F_{(n,n),s_0} & F_{(n,n),(1,1)} & F_{(n,n),(1,2)} & \cdots & F_{(n,n),(1,s_1)} & \cdots & F_{(n,n),(n,1)} & F_{(n,n),(n,2)} & \cdots & F_{(n,n),(n,s_n)} & 0 \\
1 & 1 & \cdots & 1 & 1 & 1 & \cdots & 1 & \cdots & 1 & 1 & \cdots & 1 & -1
\end{bmatrix}
\begin{bmatrix}
q_1^m \\ q_2^m \\ \cdots \\ q_{s_0}^m \\ q_{1,1}^m \\ q_{1,2}^m \\ \cdots \\ q_{1,s_1}^m \\ \cdots \\ q_{n,1}^m \\ q_{n,2}^m \\ \cdots \\ q_{n,s_n}^m \\ Q_T^m
\end{bmatrix}
=
\begin{bmatrix}
\overline{r}_1^{m-1} \\ \overline{r}_2^{m-1} \\ \cdots \\ \overline{r}_{s_0}^{m-1} \\ \overline{r}_{1,1}^{m-1} \\ \overline{r}_{1,2}^{m-1} \\ \cdots \\ \overline{r}_{1,s_1}^{m-1} \\ \cdots \\ \overline{r}_{n,1}^{m-1} \\ \overline{r}_{n,2}^{m-1} \\ \cdots \\ \overline{r}_{n,s_n}^{m-1} \\ 0
\end{bmatrix}
\tag{18}
$$

where $\overline{r}_i^{m-1} = \Delta p^m + r_i^{m-1}$, $\overline{r}_{i,j}^{m-1} = \Delta p^m + r_{i,j}^{m-1}$ and the unknown variable are

$Q_T^m, q_1^m, q_2^m, \cdots, q_{s_0}^m, q_{1,1}^m, q_{1,2}^m, \cdots, q_{1,s_1}^m, \cdots, q_{n,1}^m, q_{n,2}^m, \cdots, q_{n,s_n}^m$

Equation system of (17) and (18) are linear and nonsingular. In order to improve the solving speed and enhance the calculating accuracy, the Newton iteration method is used to solve this set of equations.

4 Model testing

Based on the model built in Section 2, fishbone and reservoir coupling software is compiled here. Then, the model is verified by inputting the data in Table 1. The horizontal well is located in the center of the reservoir and is parallel to the direction along which the reservoir extends. The main wellbore length of this well is 1,000 m. There is an equal distance between each branch. The length of each branch is 300 m. The angle between the branch and the main wellbore is 90°. Branch 1 and 3 are located on one side of the main wellbore, and branch 2 is located on the other side.

Table 1 Parameters of reservoir and horizontal well

Parameter	Value
Reservoir width, m	1000
Reservoir length, m	2000
Reservoir thickness, m	20.0
k_x, μm^2	1.0
k_y, μm^2	1.0
k_z, μm^2	1.0
Porosity, %	20
Initial reservoir pressure, MPa	22.0
Viscosity of oil, mPa·s	1.0
Compressibility, MPa^{-1}	4.0×10^{-3}
Maximum oil production, m^3/d	500
Minimum bottom hole pressure, MPa	10.0
Wellbore diameter, m	0.1
Skin factor	0

4.1 The change of the bottom hole pressure and the flux distribution

The bottom hole pressure drop is calculated with the developed model when the well produces at a constant flow rate of 500 m^3/d, as is shown in Fig. 3. In the initial production stage, the pressure wave hasn't approached to the reservoir boundaries, and the flow in the reservoir is unsteady. After about half a day, the flow in the reservoir becomes pseudo-steady. As time goes by, the pressure gradient remains almost the same.
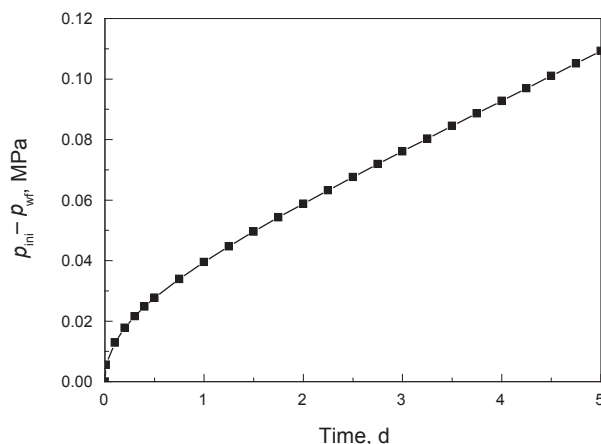

Fig. 3 Change of producing pressure drop

Fig. 4 shows the flux distribution in the wellbore after 0.01 day of production, the abscissa in the figure denotes dimensionless length x/L and ordinate in the figure denotes dimensionless inflow q_sL/Q, where x represents the distance from the point to the heel of the wellbore, L is the well length, q_s represents the inflow per unit length at a given

location, and Q represents the total well production. When the inflow along the well is uniform, the dimensionless flow rate equals one. It can be seen in Fig. 4 that the flow distribution in the three branches is completely the same. The toes of branches are closed to the main wellbore, which results in an interference between branches. The flow in the main wellbore is distributed as a "wave-shaped" form, and the location where the branch connects to the main wellbore shows as a wave trough. The flow rate at the toe is obviously smaller than that at the heel due to the interference between the toes of branches and the main wellbore. At this time, the pressure wave just propagates to the upper and lower boundaries. Therefore, the flow in each branch is only affected by the upper and lower boundaries.
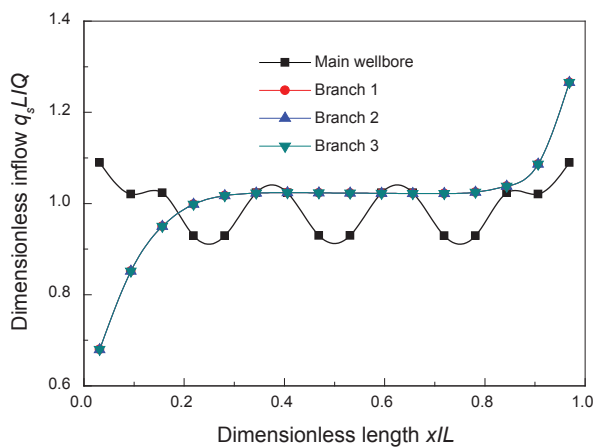

Fig. 4 Flow distribution in the wellbore in unsteady flow state at 0.01th day

Fig. 5 shows the flow distribution in the wellbore at 5th day. At this moment, the reservoir is in pseudo-steady state flow, with the pressure wave propagating to the external boundary. Since the fluid mainly comes from the x and y directions, the effect of boundary z decreases. Because of a larger contact area of the ends of the main wellbore and the branches in the reservoir, and the corresponding higher pressure support, there is a higher flow rate at these end points. The flow distribution of the main wellbore shows an irregular U-shaped curve because of the existence of the branches. The flow distribution of branch 1 almost coincides with that of branch 3 due to their space symmetrical position. Branch 2 is located at the middle of the main wellbore, the flow at the branch heel is markedly interfered, but at the branch toe the flow is weakly interfered. Therefore, the flow rate of branch 2 at the branch heel is lower than that of the branch 1, but at the branch toe, it is by contrast higher.

4.2 The effect of branch wells

Fig. 6 shows the relationship between the branch length and the flow rate of the fishbone well. A horizontal well can be considered as a fishbone well with no branch. The model is constrained by a constant bottom hole pressure of 21.0 MPa. With an increase in the branch well size, the well flow rate increases significantly at the initial production stage. After producing for a period, the impact of the branch length on the
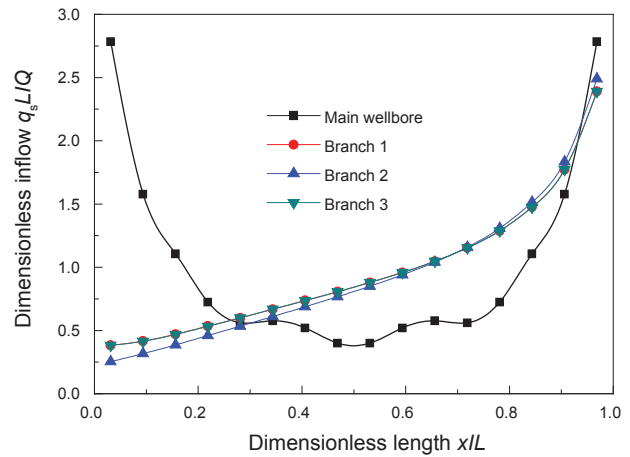

Fig. 5 Flow distribution in the wellbore in pseudo-steady flow state at 5th day

flux declines. Because the influencing area of the fishbone well expands as the branches become longer, more fluid flows into the wellbore. When the fluid near the wellbore depletes, the fluid far away from the wellbore flows into the wellbore. The resistance to the fluid flow into the wellbore is similar to that into the branches, therefore, the branch length plays a weaker role on the change of the flow rate.
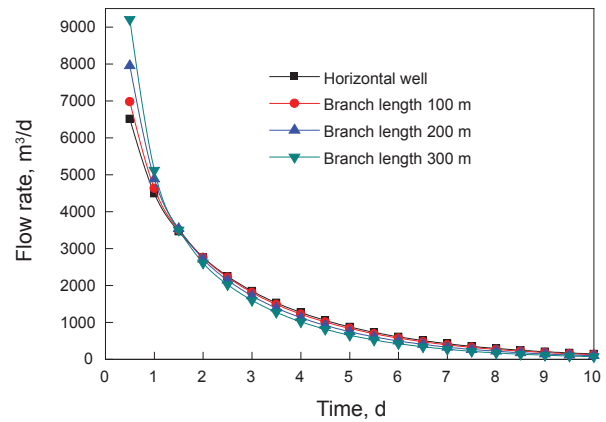

Fig. 6 The effect of the branch length on flux

Fig. 7 shows the effect of the angle between branches and the main wellbore on the flow rate when the branch length is a constant. A horizontal well can be considered that the angle between branch and the main wellbore is 0°. With an increase in the angle, the flow rate at the initial production stage increases gradually. However, at the later stage of production, the flux is only slightly influenced by the angle between the branches and the main wellbore. The reason for this is similar to that for the increased branch length. If the angle is larger than 60°, the increment of flow rate decreases.

Fig. 8 shows the effect of the branch number on the flow rate. At the beginning, the flow rate increases quickly as the branch number increases, but after a period, the flow rate changes little with an increase in the branch number. Therefore, the branch number mainly affects the flow rate of a fishbone well at the initial stage.
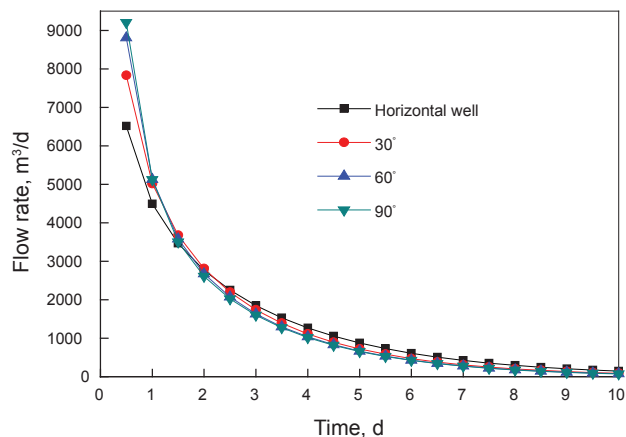
Fig. 7 The effect of the angle between branches and the main wellbore on flux
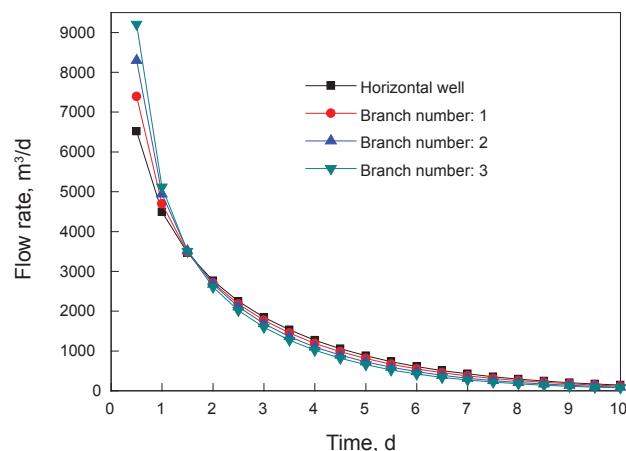

Fig. 8 The effect of the branch number on flux

5 Conclusions

1) A transient flow model for fishbone wells, which couples reservoir inflow and wellbore flow in unsteady and pseudo-steady flow state, is built. This model is constrained by flow rate or bottom hole pressure.

2) The bottom hole pressure declines quickly at the short unsteady flow stage, but the pressure drop per unit time remains the same when a steady state or a pseudo-steady state is reached in the reservoir and the wellbore.

3) During the unsteady flow (or in the unsteady flow regime), the flow curve of the main wellbore shows a "wave" shape, while the branches all present the same flow distribution pattern. Moreover, during the pseudo-steady flow, the main wellbore flow distribution seems as an irregular "U" shape, and the space-symmetric branches have the same flow distribution pattern.

4) During the initial production period, the flow rate increases significantly as the angle between the branches and the main wellbore and the length of branches increase. However, as production goes on, the length of branches and the angle between branches and the main wellbore have a gradually reduced impact on the flow rate of fishbone wells.

Acknowledgements

References

Babu D K and Odeh A S. Productivity of a horizontal well. Paper SPE 18298 presented at the SPE Annual Technical Conference and Exhibition held in Houston, October 2-5, 1988

Fan Y P, Han G Q and Yang C C. Production forecast for herringbone well and optimum configuration of lateral holes. Acta Petrolei Sinica. 2006. 27(4): 101-104 (in Chinese)

He H F, Zhang G S and Fu X. Calculating the productivity of fishbone multilateral wells with nodal method. China Offshore Oil and Gas. 2004. 16(4): 263-265 (in Chinese)

Huang S J, Cheng L S, Zhao F L, et al. Production evaluation model of fishbone well considering coupling among multi-segments flow. Journal of China University of Petroleum. 2010. 34(2): 83-88 (in Chinese)

Jasti J K, Penmatcha V R and Babu D K. Use of analytical solutions in improvement of simulator accuracy. Paper SPE 38887 presented at SPE Annual Technical Conference and Exhibition held in San Antonio, Texas, October 5-8, 1997

Jiang H Q, Ye S J, Lei Z X, et al. The productivity evaluation model and its application for finite conductivity horizontal wells in fault block reservoirs. Petroleum Science. 2011. 8(4): 530-535

Lian P Q, Cheng L S and Cui J Y. A new computation model of fractured horizontal well coupling with reservoir. International Journal for Numerical Method in Fluids. 2011. 67: 1047-1056

Li C L and Zhang S C. Productivity equation of fishbone shaped wells in steady state. Journal of Daqing Petroleum Institute. 2010. 34(1): 56-59 (in Chinese)

Liu X P, Zhang Z S and Cui G X. Inflow performance relationship of a herringbone multilateral well. Acta Petrolei Sinica. 2000. 21(6): 57-60 (in Chinese)

Ouyang L B and Aziz K. A simplified approach to couple wellbore flow and reservoir inflow for arbitrary well configurations. Paper SPE 48936 presented at the SPE Annual Technical Conference and Exhibition held in New Orleans, Louisiana, September 27-30, 1998

Penmatcha V R and Aziz K. Comprehensive reservoir/wellbore model for horizontal wells. Paper SPE 39521 presented at the SPE India Oil and Gas Conference and Exhibition held in New Delhi, India, February 17-19, 1998

Salas J R, Clifford P J and Jenkins D P. Multilateral well performance prediction. Paper SPE 35711 presented at the Western Regional Meeting held in Anchorage, Alaska, May 22-24, 1996

Wang X D, Yu G D and Li Z P. Productivity of horizontal wells with complex branches. Petroleum Exploration and Development. 2006. 33(6): 729-733 (in Chinese)

Wang Z M, Wei J G, Zhang J, et al. Optimization of perforation distribution for horizontal wells based on genetic algorithms. Petroleum Science. 2010. 7(3): 232-238

Ye S J, Jiang H Q, Zhu G J, et al. Productivity forecast and analysis of influence factors on herringbone well. Fault-block Oil & Gas Field. 2010. 17(3): 341-344 (in Chinese)

Yi F X, Yu C, Li S B, et al. Application of herringbone multilateral horizontal well in heavy oil reservoirs. Petroleum Exploration and Development. 2008. 35(4): 487-491 (in Chinese)

Yu X C, Guo B Y, Ai C, et al. A comparison between multi-fractured horizontal and fishbone wells for development of low-permeability field. Paper SPE 120579 presented at the 2009 SPE Asia Pacific Oil and Gas Conference and Exhibition held in Jakarta, Indonesia, August 4-6, 2009

Zhang L H, Zhao Y L, Liu Z B, et al. A novel steady-state productivity equation for horizontal wells in bottom water drive gas reservoirs. Petroleum Science. 2011. 8(1): 63-69

(Edited by Sun Yanhua)